Table V. Antiferromagnetic Exchange for M(III) Binuclear Complexes

| compd | $\mu_{eff}$ (298 K) | $-2J$, cm$^{-1}$ | ref |
|---|---|---|---|
| $[V(hedta\text{-}H)]_2^{2-}$ | 2.75 | 17.1 | this work, 3 |
| $[Fe(salen)]_2O$ | 1.87 | 190 | 18 |
| $[Fe(o\text{-}phen)]_2O^{4+}$ | 1.74-1.83 | 190-120 | 19 |
| $[Fe(hedta)]_2O^{2-}$ | 1.92 | 190 | 20c, 21c |
| $[Fe(TPP)]_2O$ | 1.86 | 200 | 22 |
| $[Fe(Dipic)(H_2O)(OH)]_2$ | 4.86 | 22.8 | 23, 21c |
| $[Fe(chel)(H_2O)(OH)]_2$ | 5.24 | 14.6 | 23 |
| $[Fe(H_2O)_4(OH)]_2^{4+}$ | | 80 | 24, 25, 32 |
| $[Cr(NH_3)_5]_2O^{4+}$ | | 140 | 25, 26 |
| $[Cr(o\text{-}phen)_2(OH)]_2^{4+}$ | | 43.8 | 27 |
| $[Cr(gly)_2(OH)]_2$ | | 8.4 | 28 |
| $[Cr(3Cl\text{-}acac)_2(OCH_3)]_2$ | | 7.3 | 29 |
| $[Cr(NH_3)_5]_2OH^{5+}$ | | 32 | 30 |

$[Cr(edda)(OH)]_2$ complex and only 2.4° less than for the E ring of $Co(edta)^-$. The strain in the E rings of $[V(hedta\text{-}H)]_2^{2-}$ is then normal for complexes of edta-like ligands. The approximately equatorial G ring set of $[V(hedta\text{-}H)]_2^{2-}$ appears to be more strained than the G rings of $Co(edta)^-$ by an average of 5.2° in the angle sum. The A rings are observed to have angle sums very close to the experimental values for E rings of comparison complexes.

**Magnetic Susceptibility of $[enH_2][V(hedta\text{-}H)]_2\cdot 2H_2O$.** The magnetic susceptibility data between 4.24 and 91.9 K are shown in Figure 5; the measured susceptibilities conform to the spin-only interaction of two $d^2$ ions with $S = 0$, 1, and 2 states as described by the Hamiltonian $-2J\mathbf{S}_1\cdot\mathbf{S}_2$. A $g$ value of 1.93 and a coupling constant of $2J = -17.1$ cm$^{-1}$ are the best fit parameters required to provide the solid curve of Figure 5 as calculated from eq 3

$$\chi_M = \frac{Ng^2\beta^2}{kT}\,\frac{\sum(S^2\ldots(-S)^2)e^{-S(S+1)J/kT}}{\sum(2S+1)e^{-S(S+1)J/kT}} \qquad (3)$$

throughout the temperature range. Therefore, the electronic spin moments of the two V(III) centers are only weakly antiferromagnetically coupled in contrast to the strong coupling observed for (hedta)FeOFe(hedta)$^{2-}$ complex of 1.92 $\mu$B for which the temperature dependence of the susceptibility suggests that $S_1 = S_2 = {}^5/_2$. A survey of transition-metal complexes which are known to be dihydroxy or dialcoxy bridged vs. those known to oxo bridged reveal $-2J$ values of about 20 cm$^{-1}$ for alcoxy-bridged units and >140 cm$^{-1}$ for oxo-bridged units. These comparisons are shown by Table V. The data for Fe(III) and Cr(III) complexes strongly support the dialcoxy structure for the $[V(hedta\text{-}H)]_2^{2-}$ complex ion.

**Acknowledgement** is made to the donors of the Petroleum Research Fund, administered by the American Chemical Society, for partial support of this work (grant for R.E.S.). We also acknowledge partial support of this work by the National Science Foundation through Grant No. CHE77-09913 for W.E.H.

**Supplementary Material Available:** Positional parameters for nonhydrogen atoms, fractional coordinates of atoms, and least-squares planes through atoms with deviations of atoms from planes are given in Tables SI, SII, and SIII (55 pages). Ordering information is given on any current masthead page.

# Reaction of Carbon Monoxide with the Coordinately Unsaturated Metal Dimer $(\mu\text{-}H)_2Rh_2[P(O\text{-}i\text{-}C_3H_7)_3]_4$ with Retention of Dimeric Form. Crystal and Molecular Structure of $Rh_2(\mu\text{-}CO)_2[P(O\text{-}i\text{-}C_3H_7)_3]_4$

**R. R. Burch,[1a] E. L. Muetterties,*[1a] A. J. Schultz,*[1b] E. G. Gebert,[1b] and Jack M. Williams*[1b]**

*Contribution from the Department of Chemistry, University of California, Berkeley, California 94720, and the Chemistry Division, Argonne National Laboratory, Argonne, Illinois 60439.* *Received December 18, 1980. Revised Manuscript Received April 6, 1981*

**Abstract:** The chemistry of $(\mu\text{-}H)_2Rh_2[P(O\text{-}i\text{-}C_3H_7)_3]_4$ with carbon monoxide is described. One equivalent of carbon monoxide irreversibly converted the dimer to $(\mu\text{-}H)_2Rh_2(\mu\text{-}CO)[P(O\text{-}i\text{-}C_3H_7)_3]_4$. The latter transformed slowly in solution to generate $Rh_2(\mu\text{-}CO)_2[P(O\text{-}i\text{-}C_3H_7)_3]_4$ and a second species presumed to be a hydride. The 30-electron $Rh_2(\mu\text{-}CO)_2[P(O\text{-}i\text{-}C_3H_7)_3]_4$ dimer reacted reversibly with carbon monoxide to give $Rh_2(\mu\text{-}CO)_2(CO)_2[P(O\text{-}i\text{-}C_3H_7)_3]_4$; no fragmentation to mononuclear metal complexes in this reaction system was observed up to 70 °C. Excess carbon monoxide did however elicit a fragmentation of the 30-electron complex, $(\mu\text{-}H)_2Rh_2(\mu\text{-}CO)[P(O\text{-}i\text{-}C_3H_7)_3]_4$. Reaction was rapid to give $HRh(CO)[P(O\text{-}i\text{-}C_3H_7)_3]_3$ and $HRh(CO)_2[P(O\text{-}i\text{-}C_3H_7)_3]_2$. The chemical and dynamic solution properties of these two mononuclear species is described; the properties of $HRh(CO)[P(O\text{-}i\text{-}C_3H_7)_3]_3$ diverge sharply from those of $HRh(CO)[P(C_6H_5)_3]_3$. From an X-ray diffraction study, the structure of $Rh_2(\mu\text{-}CO)_2[P(O\text{-}i\text{-}C_3H_7)_3]_4$ was established. In the $Rh_2(\mu\text{-}CO)_2$ framework, the rhodium atoms are separated by a distance of 2.630 (1) Å and the $Rh_2C_2$ array is not coplanar; rather the dihedral angle between the RhRh'C and RhRh'C' planes is 140.8 (6)°.

## Introduction

Polynuclear metal complexes present the possibility of defining in a formal context certain features of metal-surface chemistry. A constraint extant in the majority of known molecular metal clusters is their coordination saturation, a pervasive and significant feature that can substantially affect the nature of ligand bonding and result in reduced reactivity and enhanced potential for cluster fragmentation reactions. For these substantive issues, we have sought the synthesis of coordinately unsaturated metal clusters, compounds in which all or most of the metal atoms possess vacant coordination sites. Recently, we have described a series of co-

(1) (a) University of California, Berkeley, CA. (b) Argonne National Laboratory, Argonne, IL.

0002-7863/81/1503-5517$01.25/0 

ordinately unsaturated polynuclear complexes of the form $\{\mu\text{-}HRh[P(OR)_3]_2\}_x$.[2] These complexes have proven to be very active catalyst precursors for olefin and acetylene hydrogenation sequences. In the catalytic cycles, the polynuclear compounds are resistant to fragmentation and are responsible for the catalysis.[2] Nevertheless, excess phosphite rapidly and exothermically converted these polynuclear complexes to the stable mononuclear $HRh[P(OR)_3]_4$.[2] An analogous sequence was expected for carbon monoxide as a reactant. In fact, excess carbon monoxide did effect fragmentation to $HRh(CO)_x[P(OR)_3]_{4-x}$ species. However, 1 equiv of carbon monoxide converted the dimer to $(\mu\text{-}H)_2Rh_2(\mu\text{-}CO)[P(O\text{-}i\text{-}C_3H_7)_3]_4$ which disproportionated in solution to form, among other products $Rh_2(\mu\text{-}CO)_2[P(O\text{-}i\text{-}C_3H_7)_3]_4$, a dimer remarkably resistant to further fragmentation even in the presence of excess carbon monoxide.

## Experimental

**Reagents and Solvents.** All manipulations were carried out under an argon atmosphere in a Vacuum Atmospheres drybox or under a nitrogen atmosphere by using conventional Schlenk techniques. Toluene and pentane solvents were distilled from sodium benzophenone ketyl, and isopropyl alcohol was degassed prior to using. Toluene-$d_8$ NMR solvent was purchased from Aldrich and was distilled from sodium benzophenone ketyl. Hydrogen and carbon monoxide were used as received (Matheson). Carbon monoxide, 91.2% enriched in carbon-13, was purchased from Bio-Rad Laboratories.

**Spectroscopic and Analytical Methods.** All NMR spectra were recorded in toluene-$d_8$ solution or in toluene solution with a sealed inner capillary tube containing toluene-$d_8$. Chemical shifts are reported relative to the corresponding resonance of $(CH_3)_4Si$ for $^1H$ and $^{13}C$ NMR spectra and relative to 85% $H_3PO_4$ for $^{31}P$ NMR spectra. Proton NMR spectra were recorded at 90 MHz on a Varian EM-390 spectrometer and for FT-NMR spectra at 180 MHz or at 250 MHz on instruments by using Oxford superconducting magnets interfaced with Nicolet 1180 computers. Phosphorus-31 NMR spectra were recorded at 72.9 MHz on the 180-MHz spectrometer, while carbon-13 NMR spectra were run at 45.2 MHz or at 63.1 MHz on the 180- and 250-MHz spectrometers, respectively. Infrared spectra were recorded in toluene solution with 0.2-mm path length solution cells on a Perkin-Elmer 283 spectrophotometer. Microanalyses were carried out by Mr. Vazken H. Tashinian in the U.C. Berkeley Microanalytical Laboratory.

**Preparation of $Rh_2(\mu\text{-}CO)_2[P(O\text{-}i\text{-}C_3H_7)_3]_4$.** To a solution of 0.20 g (0.10 mmol) of $(\mu\text{-}H)_2Rh_2[P(O\text{-}i\text{-}C_3H_7)_3]_4$[2] in 4 mL of toluene in a Schlenk tube was added 5.1 mL (0.21 mmol) of carbon monoxide by using a gas-tight syringe. There was a nearly instantaneous color change from dark green to red. The solvent then was removed by vacuum distillation. The resulting oil was taken up in 4 mL of isopropyl alcohol, and the solution was then cooled to −20 °C for 3 days, at which time a crop of red, air-sensitive crystals was isolated by filtration in ~30% yield: IR $\nu$(CO) 1760 cm$^{-1}$; $^1H$ NMR +4.8 (m, 1 H, +1.2 ppm (d, $J_{H\text{-}H}$ = 6 Hz); $^{31}P\{^1H\}$ NMR AA′A″A‴XX′ pattern centered at +151.4 ppm; $^{13}C\{^1H\}$ NMR +238.2 ppm (approximate septet, which requires $J_{Rh\text{-}^{13}C} \simeq J_{P\text{-}^{13}C} \simeq 38.6$ Hz). Anal. Calcd for $C_{38}H_{84}O_{14}P_4Rh_2$: C, 41.68; H, 7.68; P, 11.33. Found: C, 42.19; H, 7.78; P, 11.32; P.[3]

**Preparation of $HRh(CO)[P(O\text{-}i\text{-}C_3H_7)_3]_3$.** A flow of CO gas (~20 mL/min) was passed over a solution of 0.25 g (0.24 mmol) of $(\mu\text{-}H)_2Rh_2[P(O\text{-}i\text{-}C_3H_7)_3]_4$ in 4 mL of toluene until all solvent had evaporated. The remaining oil was taken up in 5 mL of isopropyl alcohol, and the CO atmosphere was maintained. The solution was then cooled to −20 °C, and a small crop of yellow crystals precipitated from the red supernatant solution in ~30% yield. This compound in the crystalline state was handled for brief periods without decomposition in air and proved indefinitely stable under a carbon monoxide atmosphere: IR $\nu$(CO) 1955 cm$^{-1}$, $\nu$(Rh–H) 2020 cm$^{-1}$, $\nu(^{13}CO)$ 1910 cm$^{-1}$, $\nu$(Rh–H) 2010 cm$^{-1}$ for $HRh(^{13}CO)[P(O\text{-}i\text{-}C_3H_7)_3]_3$; line shapes and chemical shifts of the $^1H$ and $^{31}P$ NMR spectra were temperature dependent; $^1H$ NMR (+20 °C) +4.77 (m, 9 H), +1.25 ppm (d, $J_{H\text{-}H}$ = 6.0 Hz, 54 H), −11.20 ppm (quin, $J_{Rh\text{-}H} \approx J_{P\text{-}H}$ = 5.7 Hz, 1 H); $^1H$ NMR (−70 °C) +4.77 (m, 9 H), +1.25 (d, $J_{H\text{-}H}$ = 6.0 Hz, 54 H), −11.05 ppm (d, $J_{Rh\text{-}H}$ = 5.7 Hz, $\omega_{1/2}$ = 6.0 Hz, 1 H); $^1H\{^{31}P\}$ (20 °C) +4.77 (m, 9 H), +1.25 (d, $J_{H\text{-}H}$ = 6.0 Hz, 54 H), −11.05 ppm (d, $J_{Rh\text{-}H}$ = 5.7 Hz, 1 H); $^{31}P\{^1H$ alkyl$\}$ NMR (+25 °C) +116.8 ppm (d of d, $J_{Rh\text{-}P}$ = 226 Hz, $J_{P\text{-}H}$ = 5.7 Hz); $^{31}P\{^1H\}$ NMR (−70 °C) +160.4 ppm (d, $J_{Rh\text{-}P}$ = 226 Hz); $^{13}C\{^1H\}$ NMR (+20 °C) +214.3 ppm (d of q, $J_{Rh\text{-}^{13}C}$ = 52.5 Hz, $J_{P\text{-}^{13}C}$ = 13.1 Hz). Anal. Calcd for $C_{28}H_{64}O_{10}P_3Rh$: C, 44.44; H, 8.46; P, 12.30. Found: C, 44.54; H, 8.45; P, 11.95.

**Spectroscopic Monitoring of the Reactions of $(\mu\text{-}H)_2Rh_2[P(O\text{-}i\text{-}C_3H_7)_3]_4$ and of $(H)(\mu\text{-}H)_3Rh_2[P(O\text{-}i\text{-}C_3H_7)_3]_4$ with CO.** Proton NMR monitoring of the reaction of $(\mu\text{-}H)_2Rh_2[P(O\text{-}i\text{-}C_3H_7)_3]_4$ with carbon monoxide was carried out by the following procedure. To a 60-mL reaction tube with a 5-mm tube attached to the side was added 0.02 g (0.019 mmol) of $(\mu\text{-}H)_2Rh_2[P(O\text{-}i\text{-}C_3H_7)_3]_4$. Approximately 0.5 mL of toluene-$d_8$ was introduced by vacuum distillation, and the tube was filled with 0.7 atm of carbon monoxide. The solution was stirred magnetically for the appropriate amount of time, and then the solution was poured into the NMR tube side arm, which was then torch-sealed; the CO atmosphere was thereby maintained. A similar procedure was used for reactions of $(H)(\mu\text{-}H)_3Rh_2[P(O\text{-}i\text{-}C_3H_7)_3]_4$ except that hydrogen was introduced after the solvent addition to generate $(H)(\mu\text{-}H)_3Rh_2[P(O\text{-}i\text{-}C_3H_7)_3]_4$.[2] The resulting solution was then frozen, and the excess $H_2$ was removed by evacuation. In some reactions, $H_2$ and CO mixtures were introduced simultaneously.

For infrared monitoring, the appropriate solution was generated in a Schlenk tube which was then transferred by means of a metal cannula to the $N_2$-flushed solution infrared cell which had serum caps covering the ports.

**X-ray Crystal Structure of $Rh_2(\mu\text{-}CO)_2[P(O\text{-}i\text{-}C_3H_7)_3]_4$.** The crystal selected for data collection had approximate dimensions of 0.50 × 0.36 × 0.32 mm and was sealed in a thin-walled glass capillary under nitrogen. With the crystal mounted in a general orientation, data were collected on a Syntex $P2_1$ diffractometer equipped with a graphite monochromator. Because the quality of the Bragg peak profiles always decreased rather than increased on cooling to −100 °C, all data were measured at room temperature. The unit cell parameters obtained by least-squares fit of 15 automatically centered reflections in the range $20° < 2\theta < 25°$ (Mo K$\bar{\alpha}$ x-radiation, $\lambda$ = 0.71069 Å) were $a$ = 24.307 (5) Å, $b$ = 12.191 (3) Å, $c$ = 19.523 (4) Å, $\beta$ = 94.25 (2)°, and $V$ = 5769 (2) Å$^3$. The data revealed systematic extinctions consistent with $C$-centered monoclinic space groups $Cc$ [$C_s^4$—No. 9][4a] and $C2/c$ [$C_{2h}^6$—No. 15].[4a] The centrosymmetric space group $C2/c$ was chosen initially on the basis of the presence of certain Harker vectors in the Patterson synthesis map[5] and the statistical distribution of intensities obtained from MULTAN.[6] The satisfactory structure solution ultimately obtained supports this choice. With a molecular weight of 1094.82 and $Z$ = 4, $\rho_c$ is 1.261 g/cm$^3$.

Intensity data were collected for two octants ($+h$, $+k$, $\pm l$) of $C$-centered intensity data out to $2\theta = 45°$ by using the $\theta$–$2\theta$ step-scan mode with variable scan rates of 2.0–29.3° min$^{-1}$. The data were corrected for absorption ($\mu_{calcd}$ = 7.180 cm$^{-1}$) with transmission coefficients ranging from 0.78 to 0.81. Variances of $F_o^2$ were calculated by using the expression $\sigma^2(F_o^2) = \sigma_c^2(F_o^2) + (0.03F_o^2)^2$, where $\sigma_c^2(F_o^2)$ is determined from counting statistics.

The coordinates of the independent rhodium atom were obtained from a Patterson synthesis map[5] and from direct methods with MULTAN.[6] All other nonhydrogen atom positions were determined by using standard Fourier and least-squares refinement procedures. Corrections for anomalous scattering were included in the structure factor calculations.[4b] Only when anisotropic thermal parameters were used did all bond lengths and angles fall within expected ranges. The positions of all hydrogen atoms were calculated or obtained from a difference Fourier map. At this stage in the refinement, each $\sigma(F_o)$ was incremented by a value of 100 since many unobserved data so characterized from inspection of their peak profiles were being treated as observed data due to underestimated standard deviations. However, because many of the hydrogen atoms shifted to unreasonable positions, they were removed from the final least-squares refinement. Although the $R$ factors increased, many of the nonhydrogen interatomic distances shifted to more chemically reasonable values (e.g., the C(7)–C(8) bond distance changed from 1.27 (2) to 1.44 (2) Å). Furthermore, because of very large thermal motion of the methyl group carbon atoms, the inclusion of hydrogen atoms with calculated positions is not easily justified. The parameters given in Table I were obtained from the final least-squares cycle using all 3802 reflections. With use of the 3802 independent data, the discrepancy indices were found to be $R(F_o)$ = 0.094, $R(F_o^2)$ = 0.086, and $R_w(F_o^2)$ = 0.112, with $\sigma_1$ = 1.36. With use of the 2796 data were $F_o^2 > \sigma(F_o^2)$, $R(F_o)$ = 0.064, $R(F_o^2)$ = 0.082, and $R_w(F_o^2)$ = 0.110, with $\sigma_1$ = 1.57. The highest peak

(2) Sivak, A. J.; Muetterties, E. L. *J. Am. Chem. Soc.* **1979**, *101*, 4878.

(3) Some difficulty was encountered in obtaining a satisfactory analysis of $Rh_2(\mu\text{-}CO)_2[P(O\text{-}i\text{-}C_3H_7)_3]_4$ due to the reactivity of this material. This analysis represents the best set of three analyses.

(4) (a) "International Tables for X-Ray Crystallography"; Kynoch Press: Birmingham, England, 1969; Vol. I. (b) *Ibid.* 1974; Vol. IV.

(5) Details of data reduction and structure refinement programs have been reported previously; see: Schultz, A. J.; Underhill, A. E.; Williams, J. M. *Inorg. Chem.* **1978**, *17*, 1313.

(6) Declercq, J. P.; Germain, G.; Main, P.; Woolfsen, M. M. *Acta Crystallogr., Sect. A* **1973**, *A29*, 231.

Table I. Final Positional[a] and Thermal[b] Parameters for $Rh_2(\mu\text{-}CO)_2[P(O\text{-}i\text{-}C_3H_7)_3]_4$

| ATOM | X | Y | Z | U11 | U22 | U33 | U12 | U13 | U23 |
|---|---|---|---|---|---|---|---|---|---|
| RH | 0.04497(2) | 0.17094(4) | 0.21648(3) | 0.0389(4) | 0.0776(4) | 0.0775(4) | 0.0072(4) | 0.0190(3) | 0.0002(4) |
| P1 | 0.05149(9) | 0.2993(2) | 0.1342(1) | 0.112(2) | 0.079(1) | 0.099(2) | -0.008(1) | 0.033(1) | 0.005(1) |
| P2 | 0.1267(1) | 0.0869(3) | 0.2030(1) | 0.138(2) | 0.181(3) | 0.100(2) | 0.070(2) | 0.041(2) | 0.010(2) |
| O1 | 0.1104(2) | 0.3554(5) | 0.1411(3) | 0.139(5) | 0.129(5) | 0.145(5) | -0.041(4) | 0.054(4) | -0.004(4) |
| O2 | 0.0391(3) | 0.2766(5) | 0.0552(3) | 0.203(6) | 0.116(4) | 0.093(4) | -0.010(4) | 0.020(4) | 0.026(4) |
| O3 | 0.0150(3) | 0.4038(4) | 0.1395(3) | 0.170(6) | 0.083(4) | 0.181(6) | 0.021(4) | 0.072(5) | 0.029(4) |
| O4 | 0.1533(3) | 0.0940(5) | 0.1374(3) | 0.162(6) | 0.185(6) | 0.123(4) | 0.058(5) | 0.068(4) | 0.013(4) |
| O5 | 0.1756(4) | 0.1140(13) | 0.2643(5) | 0.153(8) | 0.53(2) | 0.142(7) | 0.18(1) | -0.002(6) | -0.05(1) |
| O6 | 0.1269(6) | -0.0483(11) | 0.2134(5) | 0.34(2) | 0.26(1) | 0.21(1) | 0.21(1) | 0.17(1) | 0.11(1) |
| C1 | 0.1226(5) | 0.4518(9) | 0.0930(6) | 0.22(1) | 0.13(1) | 0.21(1) | -0.054(9) | 0.12(1) | 0.009(9) |
| C2 | 0.1310(7) | 0.5480(11) | 0.1487(9) | 0.39(2) | 0.17(1) | 0.32(2) | -0.14(1) | 0.22(2) | -0.09(1) |
| C3 | 0.1770(6) | 0.4215(11) | 0.0647(7) | 0.22(1) | 0.23(1) | 0.26(1) | -0.09(1) | 0.15(1) | -0.03(1) |
| C4 | 0.0414(6) | 0.1675(9) | 0.0198(5) | 0.25(1) | 0.11(1) | 0.113(7) | -0.008(9) | 0.029(8) | -0.018(7) |
| C5 | 0.0925(6) | 0.1711(10) | -0.0220(5) | 0.28(1) | 0.22(1) | 0.138(9) | 0.05(1) | 0.09(1) | 0.001(9) |
| C6 | -0.0126(7) | 0.1593(12) | -0.0256(6) | 0.29(2) | 0.23(1) | 0.135(9) | -0.07(1) | -0.05(1) | 0.011(9) |
| C7 | -0.0447(6) | 0.4104(9) | 0.1355(7) | 0.19(1) | 0.14(1) | 0.19(1) | 0.091(9) | 0.09(1) | 0.073(8) |
| C8 | -0.0685(8) | 0.4304(20) | 0.0646(9) | 0.30(2) | 0.48(3) | 0.21(2) | 0.19(2) | 0.02(1) | 0.04(2) |
| C9 | -0.0598(8) | 0.4952(16) | 0.1815(9) | 0.35(2) | 0.37(2) | 0.25(2) | 0.25(2) | 0.02(2) | -0.03(2) |
| C10 | 0.2054(7) | 0.0349(16) | 0.1246(7) | 0.13(1) | 0.31(2) | 0.18(1) | 0.12(1) | 0.08(1) | 0.01(1) |
| C11 | 0.1904(8) | -0.0410(16) | 0.0646(8) | 0.35(2) | 0.37(3) | 0.20(1) | 0.21(2) | 0.06(1) | -0.09(1) |
| C12 | 0.2450(6) | 0.1204(17) | 0.1037(9) | 0.19(1) | 0.38(3) | 0.27(2) | 0.06(2) | 0.14(1) | 0.02(2) |
| C13 | 0.1773(5) | 0.2067(16) | 0.3099(8) | 0.115(9) | 0.33(2) | 0.15(1) | 0.01(1) | 0.026(8) | -0.01(1) |
| C14 | 0.2150(8) | 0.2920(19) | 0.2812(10) | 0.23(2) | 0.51(3) | 0.30(2) | -0.19(2) | 0.01(2) | 0.00(2) |
| C15 | 0.1947(6) | 0.1630(19) | 0.3812(8) | 0.22(2) | 0.51(3) | 0.14(1) | 0.03(2) | -0.02(1) | -0.01(2) |
| C16 | 0.1006(6) | -0.1082(14) | 0.2585(11) | 0.19(1) | 0.15(1) | 0.26(2) | 0.05(1) | 0.01(1) | -0.08(1) |
| C17 | 0.1384(8) | -0.1819(16) | 0.2957(9) | 0.29(2) | 0.32(2) | 0.26(2) | 0.10(2) | 0.10(2) | 0.16(2) |
| C18 | 0.0681(15) | -0.1841(15) | 0.2205(18) | 0.92(7) | 0.15(1) | 0.61(5) | 0.02(2) | -0.40(6) | -0.00(2) |
| C | 0.0348(3) | 0.1283(6) | 0.3144(4) | 0.111(6) | 0.102(6) | 0.091(6) | 0.029(5) | 0.015(5) | -0.004(5) |
| O | 0.0539(3) | 0.1014(6) | 0.3668(3) | 0.155(5) | 0.192(6) | 0.088(4) | 0.067(5) | 0.002(4) | 0.021(4) |

[a] $x$, $y$ and $z$ are fractional coordinates. [b] Anisotropic temperature factors of the form $\exp[-2\pi^2(a^{*2}U_{11}h^2 + \ldots + 2a^*b^*U_{12}hk + \ldots)]$.

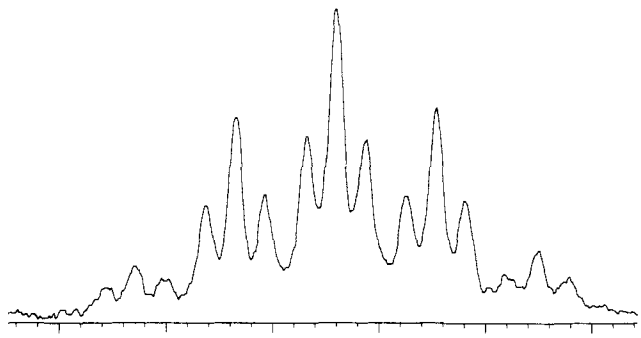

**Figure 1.** 180-MHz $^1H$ NMR spectrum in the hydride region of $(\mu\text{-}H)_2Rh_2(\mu\text{-}CO)[P(O\text{-}i\text{-}C_3H_7)_3]_4$.

on the final difference Fourier map corresponded to 0.63 $e^-/Å^3$. We attribute the relatively high $R$ factors and standard deviations in the final results to somewhat poor crystal quality, although it was the best crystal tested, and to high thermal motion associated with the room-temperature data set.

## Results and Discussion

Reaction of $(\mu\text{-}H)_2Rh_2[P(O\text{-}i\text{-}C_3H_7)_3]_4$ with 1 equiv of carbon monoxide at 20 °C was signaled by an immediate color change from dark green to red. This initial product was not successfully isolated because of its reactivity, but the combination of NMR and IR spectroscopy provided an unequivocal representation as $(\mu\text{-}H)_2Rh_2(\mu\text{-}CO)[P(O\text{-}i\text{-}C_3H_7)_3]_4$. The CO stretching frequency was at 1805 $cm^{-1}$, characteristic of a bridging carbonyl ligand. The $^1H$ NMR spectrum, shown in Figure 1, was temperature invariant from −80 to +25 °C, and was a quintet (equivalent coupling to four phosphorus nuclei) of triplets (equivalent coupling to two rhodium nuclei) (see Figure 1), that reduced in the $^1H\{^{31}P\}$ experiment to a triplet resonance.[7] Consistently, the $^{13}C$ NMR spectrum for the $^{13}C$ CO-enriched complex was a quintet of triplets.[7] Hence, the first spectroscopically observable species in the reaction of $(\mu\text{-}H)_2Rh_2[P(O\text{-}i\text{-}C_3H_7)_3]_4$ and carbon monoxide was $(\mu\text{-}H)_2Rh_2(\mu\text{-}CO)[P(O\text{-}i\text{-}C_3H_7)_3]_4$. This step appeared to be irreversible in that evacuation at 0.1 torr led to no discernable loss of carbon monoxide.

In solution, $(\mu\text{-}H)_2Rh_2(\mu\text{-}CO)[P(O\text{-}i\text{-}C_3H_7)_3]_4$ slowly converted at −25 °C to a mixture of two complexes. One was a new carbonyl bridged dimer, $Rh_2(\mu\text{-}CO)_2[P(O\text{-}i\text{-}C_3H_7)_3]_4$, which was isolated, fully characterized, and structurally defined (see later crystallographic discussion). The other product displayed a weak infrared absorption at 1985 $cm^{-1}$ which could be ascribed to a terminal Rh–H stretching vibration. We assumed that this other product of "disproportionation" was the tetrahydride, $H(\mu\text{-}H)_3Rh_2[P(O\text{-}i\text{-}C_3H_7)_3]_4$ as implied in eq 1. However, although the tetrahydride

$$2(\mu\text{-}H)_2Rh_2(\mu\text{-}CO)[P(O\text{-}i\text{-}C_3H_7)_3]_4 \rightarrow Rh_2(\mu\text{-}CO)_2[P(O\text{-}i\text{-}C_3H_7)_3]_4 + (H)(\mu\text{-}H)_3Rh_2[P(O\text{-}i\text{-}C_3H_7)_3]_4 \quad (1)$$

is a well-defined complex derived from $(\mu\text{-}H)_2Rh_2[P(O\text{-}i\text{-}C_3H_7)_3]_4$ and hydrogen[2] we could obtain no unambiguous spectroscopic evidence that this tetrahydride complex was the other product of this reaction.

Carbon monoxide reacted with the 30-electron dimer, $Rh_2(\mu\text{-}CO)_2[P(O\text{-}i\text{-}C_3H_7)_3]_4$, to give the 34-electron complex $Rh_2(\mu\text{-}CO)_2(CO)_2[P(O\text{-}i\text{-}C_3H_7)_3]_4$ which was characterized by infrared and NMR spectroscopy.[8] This CO addition was readily reversed by momentary evacuation of these solutions. Hence, the thermal reaction sequence for this complex was facile reversible CO addition (eq 2). Such a reaction sequence had been observed before

$$Rh_2(\mu\text{-}CO)_2[P(O\text{-}i\text{-}C_3H_7)_3]_4 + 2CO \rightleftharpoons Rh_2(\mu\text{-}CO)_2(CO)_2[P(O\text{-}i\text{-}C_3H_7)_3]_4 \quad (2)$$

for the formally analogous phosphine compound $Rh_2(\mu\text{-}CO)_2[P(C_6H_5)_3]_4$.[9] Further reaction of carbon monoxide with the phosphite complex did not occur up to 70 °C over the course of several hours; thus, the tetracarbonyl is quite resistant to fragmentation. This behavior diverges sharply from that of $(\mu\text{-}H)_2Rh_2(\mu\text{-}CO)[P(O\text{-}i\text{-}C_3H_7)_3]_4$ and its reactions with excess carbon monoxide as discussed below.

Excess carbon monoxide did elicit a fragmentation of the 30-electron complex $(\mu\text{-}H)_2Rh_2(\mu\text{-}CO)[P(O\text{-}i\text{-}C_3H_7)_3]_4$. This reaction was rapid and was visually evident in a change in solution color to an orange-yellow cast. Formed in this relatively rapid reaction was $HRh(CO)[P(O\text{-}i\text{-}C_3H_7)_3]_3$, a coordinately saturated species

(7) The resonance in the hydride region of the $^1H$ NMR spectrum was centered at −9.05 ppm relative to $(CH_3)_4Si$, with $J_{Rh\text{-}H} = 14.1$ Hz and $J_{P\text{-}H} = 47.2$ Hz. The carbonyl carbon resonance in the $^{13}C\{^1H\}$ NMR spectrum was centered at +233.0 ppm, with $J_{^{13}C\text{-}Rh} = 30.2$ Hz and $J_{^{13}C\text{-}P} = 42.6$ Hz.

(8) The $\nu$(CO) infrared spectrum consisted of an absorption for terminal carbonyls (1980 $cm^{-1}$) and an absorption for bridging carbonyls (1820 $cm^{-1}$). The −65 °C $^{13}C$ NMR spectrum of $Rh_2(\mu\text{-}^{13}CO)_2(^{13}CO)_2[P(O\text{-}i\text{-}C_3H_7)_3]_4$ showed two sets of complex resonances at +214 and +196 ppm.

(9) Evans, D.; Yagupsky, G.; Wilkinson, G. *J. Chem. Soc. A* **1968**, 2660.

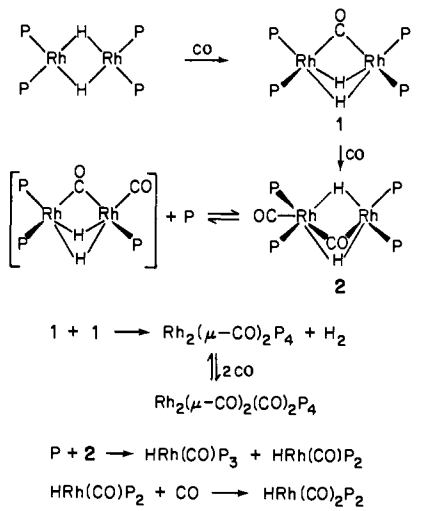


**Figure 2.** Reaction sequence for the carbon monoxide addition to $(\mu\text{-H})_2Rh_2[P(O\text{-}i\text{-}C_3H_7)_3]_4$. The formation of $(\mu\text{-CO})_2Rh_2[P(O\text{-}i\text{-}C_3H_7)_3]_4$ from $(\mu\text{-H})_2Rh_2[P(O\text{-}i\text{-}C_3H_7)_3]_4$ requires the formation of $H_2$ and the elements of $(\mu\text{-H})_2Rh_2[P(O\text{-}i\text{-}C_3H_7)_3]_4$. Hydrogen is known to react with the latter rhodium dimer to form $(H)(\mu\text{-H})_3Rh_2[P(O\text{-}i\text{-}C_3H_7)_3]_4$. Thus, the hydrogen produced in the reaction depicted in this figure was likely present as $(H)(\mu\text{-H})_3Rh_2[P(O\text{-}i\text{-}C_3H_7)_3]_4$, making the overall transformation a disproportionation reaction: $2[(\mu\text{-H})_2Rh_2[P(O\text{-}i\text{-}C_3H_7)_3]_4] \rightarrow (\mu\text{-CO})_2Rh_2[P(O\text{-}i\text{-}C_3H_7)_3]_4 + (H)(\mu\text{-H})_3Rh_2[P(O\text{-}i\text{-}C_3H_7)_3]_4$.

fully characterized by analysis and spectroscopic data described in the Experimental Section. The second spectroscopically detected species from the CO scission of $(\mu\text{-H})_2Rh_2(\mu\text{-CO})[P(O\text{-}i\text{-}C_3H_7)_3]_4$ was $HRh(CO)_2[P(O\text{-}i\text{-}C_3H_7)_3]_2$ whose $^1H$ NMR spectrum at +20 °C was a doublet of triplets which reduced to a doublet in the $^1H\{^{31}P\}$ NMR.[10] The $^{13}C\{^1H\}$ NMR spectrum in the carbonyl region was a doublet of triplets. These two compounds, $HRh(CO)[P(O\text{-}i\text{-}C_3H_7)_3]_3$ and $HRh(CO)_2[P(O\text{-}i\text{-}C_3H_7)_3]_2$, were formed in nearly equal proportions along with a set of other species. The last set was clearly indicated by the infrared and NMR data although the data did not permit a clear delineation of structure or composition.[12]

Scheme I

$$HRh(CO)[P(C_6H_5)_3]_3 \rightleftharpoons HRh(CO)[P(C_6H_5)_3]_2 + P(C_6H_5)_3$$
$$\downarrow\uparrow CO$$
$$HRh(CO)_2[P(C_6H_5)_3]_2$$
$$H_2 \downarrow\uparrow CO$$
$$Rh_2(\mu\text{-CO})_4[P(C_6H_5)_3]_4$$
$$\downarrow\uparrow (-CO)$$
$$Rh_2(\mu\text{-CO})_2[P(C_6H_5)_3]_4$$

Formation of $HRh(CO)[P(O\text{-}i\text{-}C_3H_7)_3]_3$ from the CO reaction with $(\mu\text{-H})_2Rh_2(\mu\text{-CO})[P(O\text{-}i\text{-}C_3H_7)_3]_4$ requires a phosphite ligand dissociation process. A possible reaction sequence is outlined in Figure 2 where CO first adds to the 30-electron dimer to give a species, **2**, that is isostructural with $H(\mu\text{-H})_3Rh_2[P(O\text{-}i\text{-}C_3H_7)_3]_4$.[2] We suggest that phosphite dissociation occurs in this 32-electron CO adduct. Then, phosphite attack of the dimer **2** should be fast to form the mononuclear monocarbonyl. The high rate of this reaction unfortunately precluded infrared monitoring of the reaction and hence spectroscopic evidence for the putative intermediate **2** in this conversion could not be developed.

There was a $^1H$ NMR chemical shift temperature dependence for $HRh(CO)[P(O\text{-}i\text{-}C_3H_7)_3]_3$ which implicated a ligand dissociation and recombination process that was fast relative to the NMR time scale. Here it is tempting to invoke a dissociation of a phosphite ligand to form $HRh(CO)[P(O\text{-}i\text{-}C_3H_7)_3]_2$ analogous to that reported for $HRh(CO)[P(C_6H_5)_3]_3$.[9] Rather, in sharp contrast, the carbonyl group is the labile ligand in $HRh(CO)[P(O\text{-}i\text{-}C_3H_7)_3]_3$, and an interconversion between $HRh(CO)[P(O\text{-}i\text{-}C_3H_7)_3]_3$ and $HRh(CO)[P(O\text{-}i\text{-}C_3H_7)_3]_2$ was not observed. Evacuation at 0.1 torr of toluene solutions of $HRh(CO)[P(O\text{-}i\text{-}C_3H_7)_3]_3$ induced a yellow to red color change which was accompanied in the infrared spectrum by the disappearance of the absorption at 2020 and 1955 $cm^{-1}$ for the starting material and by the appearance of a new absorption at 2000 $cm^{-1}$. Addition of CO at this point regenerated $HRh(CO)[P(O\text{-}i\text{-}C_3H_7)_3]_3$, while addition of $^{13}CO$ generated $HRh(^{13}CO)[P(O\text{-}i\text{-}C_3H_7)_3]_3$ ($\nu(^{13}CO)$ = 1910 $cm^{-1}$). The monocarbonyl $HRh(CO)[P(O\text{-}i\text{-}C_3H_7)_3]_3$ also reacted rapidly with excess $P(OCH_3)_3$ to afford the spectroscopically identified $HRh[P(OCH_3)_3]_4$ and other metal hydrides whose similar chemical shifts and coupling constants observed in the hydride region of the $^1H$ NMR spectrum show them to be $HRh[P(O\text{-}i\text{-}C_3H_7)_3][P(OCH_3)_3]_3$ and $HRh[P(O\text{-}i\text{-}C_3H_7)_3]_2[P(OCH_3)_3]_2$.[2] No infrared absorption for a metal-bound carbonyl could be found in these reaction solutions. All these data establish that loss of CO from $HRh(CO)[P(O\text{-}i\text{-}C_3H_7)_3]_3$ to give $HRh[P(O\text{-}i\text{-}C_3H_7)_3]_3$ is a facile process.

The products $HRh(CO)[P(O\text{-}i\text{-}C_3H_7)_3]_3$ and $HRh(CO)_2[P(O\text{-}i\text{-}C_3H_7)_3]_2$ were found in the reaction of $(\mu\text{-H})_2Rh_2[P(O\text{-}i\text{-}C_3H_7)_3]_4$ and excess carbon monoxide even in the presence of an excess of hydrogen. For example, $(\mu\text{-H})_2Rh_2[P(O\text{-}i\text{-}C_3H_7)_3]_4$ as well as $(H)(\mu\text{-H})_3Rh_2[P(O\text{-}i\text{-}C_3H_7)_3]_4$ reacted rapidly with a 3:1 mixture of hydrogen and carbon monoxide at 1 atm at 20 °C to form the yellow solutions of $HRh(CO)[P(O\text{-}i\text{-}C_3H_7)_3]_3$, $HRh(CO)_2[P(O\text{-}i\text{-}C_3H_7)_3]_2$, and the other rhodium phosphite species. The products were formed in essentially the same proportions as in the reaction of $(\mu\text{-H})_2Rh_2[P(O\text{-}i\text{-}C_3H_7)_3]_4$ with carbon monoxide in the absence of hydrogen. Thus, the above results show that carbon monoxide is better able to compete for $(\mu\text{-H})_2Rh_2[P(O\text{-}i\text{-}C_3H_7)_3]_4$ than is hydrogen.

The compound $Rh_2(\mu\text{-CO})_2[P(O\text{-}i\text{-}C_3H_7)_3]_4$ also reacted with $H_2$ slowly and irreversibly over the course of 24 h to yield a green solution in which no metal hydride could be detected by NMR.[13] This behavior contrasts with that of the phosphine analogue $Rh_2(\mu\text{-CO})_2[P(C_6H_5)_3]_4$ for which hydrogen effected the dimer

(10) The 250-MHz $^1H$ NMR chemical shift in the hydride region was at −10.0 ppm with $J_{Rh\text{-}H}$ = 8.7 Hz and $J_{P\text{-}H}$ = 63.2 Hz. When the sample was cooled, the pair of resonances at the center of this triplet of doublet pattern broadened and this chemical shift moved farther downfield while a new resonance of low intensity appeared at −12.5 ppm. At −65 °C, the spectrum consisted of a doublet of doublets at −9.30 ppm and a resonance of low intensity at −12.50 ppm which had doublet character. These spectra clearly demonstrate the presence of two isomers. Such isomerism has been observed in the analogous iridium compounds $HIr(CO)_2[P(p\text{-}C_6H_4CH_3)_3]_2$,[11] but the present data do not allow an unambiguous assignment of the isomers for the rhodium phosphite complexes. The mass spectrum showed a parent ion at 576 amu as well as ions at 548 and 520 amu for the fragments $HRh(CO)[P(O\text{-}i\text{-}C_3H_7)_3]_2^+$ and $HRh[P(O\text{-}i\text{-}C_3H_7)_3]_2^+$, respectively. The infrared spectrum of $HRh(CO)_2[P(O\text{-}i\text{-}C_3H_7)_3]_2$, which could not be obtained free from the other products formed in this reaction, showed the following absorptions: 2020 (w), 2000 (m), 1985 (w, sh), 1850 (s), 1820 (m), and 1775 (m) $cm^{-1}$.[12]

(11) Meakin, P.; Muetterties, E. L.; Jesson, J. P. *J. Am. Chem. Soc.* **1972**, *94*, 5271.

(12) The $^{13}C$ NMR spectrum of the solution from the reaction of excess $^{13}CO$ with $(\mu\text{-H})_2Rh_2[P(O\text{-}i\text{-}C_3H_7)_3]_4$ had, in addition to resonances for the two mononuclear metal hydrides, a triplet at +214.5 ppm with a coupling constant of 12.3 Hz and three broad resonances at +187.9, +214.9, and +237.0 ppm. Upon being cooled to −60 °C, these broad resonances sharpened but were still not straightforwardly interpretable. The $^{31}P\{^1H\}$ NMR spectrum showed three sharp resonances at −1.7, +0.7, and +4.6 ppm as well as a complex set in the region +118 to +145 ppm. No clear coupling pattern was evident. The infrared spectrum in the carbonyl region showed in addition to absorptions for the mononuclear products absorptions in the bridging carbonyl region at 1830 (w), 1770 (m), and 1740 (w, sh) $cm^{-1}$. The mass spectra of samples prepared from these solutions showed the pattern for the two mononuclear products and also was particularly distinguished by an intense peak at 996 amu and one at 952 amu corresponding to loss of a $C_3H_7$ group from the ion at 996 amu. Peaks at higher amu were also evident. Thus $(\mu\text{-H})_2Rh_2(\mu\text{-CO})[P(O\text{-}i\text{-}C_3H_7)_3]_4$ reacts with CO to form $HRh(CO)[P(O\text{-}i\text{-}C_3H_7)_3]_3$, $HRh(CO)_2[P(O\text{-}i\text{-}C_3H_7)_3]_2$, and some other species which must be polynuclear and phosphorus ligand deficient (to be consistent with the reaction stoichiometry).

(13) The infrared spectrum showed absorptions at 2013 (m), 1985 (sh), 1940 (w), 1810 (br, m), and 1750 (m) $cm^{-1}$.

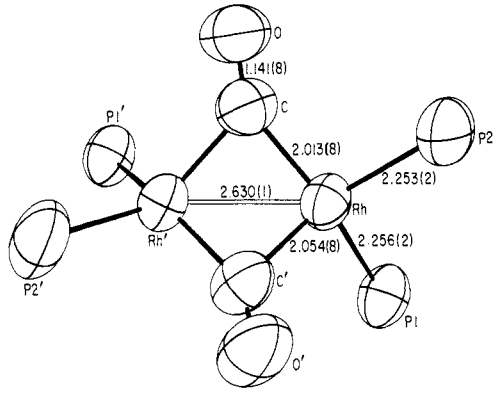


**Figure 3.** ORTEP drawing of $Rh_2(\mu\text{-}CO)_2[P(O\text{-}i\text{-}C_3H_7)_3]_4$. The isopropoxy groups have been eliminated for clarity.

fragmentation reaction to form $HRh(CO)_2[P(C_6H_5)_3]_2$ (in the presence of excess carbon monoxide). Thus, the failure of $Rh_2(\mu\text{-}CO)_2[P(O\text{-}i\text{-}C_3H_7)_3]_4$ to form $(\mu\text{-}H)_2Rh_2[P(O\text{-}i\text{-}C_3H_7)_3]_4$ in the reaction with hydrogen establishes that the reaction sequence which leads to the formation of $Rh_2(\mu\text{-}CO)_2[P(O\text{-}i\text{-}C_3H_7)_3]_4$ must be an irreversible one.

Unsuccessful were attempts to reduce carbon monoxide by reaction of $(\mu\text{-}H)_2Rh_2[P(O\text{-}i\text{-}C_3H_7)_3]_4$ with 3:1 mixtures of hydrogen and carbon monoxide at 1 atm at 90 °C in octane solution for up to 40 h. Acetone, propane, as well as small amounts of methane, ethane, butane, and isobutane were detected by gas chromatography and gas chromatography–mass spectrometry in the vapor phase above the reaction solutions; but deuterium and [$^{13}$C]carbon monoxide labeling studies showed that these volatile hydrocarbons arise from decomposition of the $P(O\text{-}i\text{-}C_3H_7)_3$ ligand. No alcohols were detected in these reactions.

The decomposition of $(\mu\text{-}H)_2Rh_2(\mu\text{-}CO)[P(O\text{-}i\text{-}C_3H_7)_3]_4$ to mononuclear products was also effected by other reagents. Addition of 1 equiv of $H_3B{\cdot}OC_4H_8$ to solutions of $(\mu\text{-}H)_2Rh_2(\mu\text{-}CO)[P(O\text{-}i\text{-}C_3H_7)_3]_4$ resulted in the immediate formation of $HRh(CO)[P(O\text{-}i\text{-}C_3H_7)_3]_3$, $HRh(CO)_2[P(O\text{-}i\text{-}C_3H_7)_3]_2$, and the other rhodium–carbonyl-containing products.

In summary, it is important and instructive to explicity enumerate the distinctive chemical differences between the rhodium phosphite chemistry described above and that based on $HRh(CO)[P(C_6H_5)_3]_3$.[9] First, there is no triphenylphosphine analogue of the key dimeric rhodium hydride complex $(\mu\text{-}H)_2Rh_2[P(O\text{-}i\text{-}C_3H_7)_3]_4$ and no analogue of $(\mu\text{-}H)_2Rh_2(\mu\text{-}CO)[P(O\text{-}i\text{-}C_3H_7)_3]_4$. There is a purely formal analogy in a narrow region of chemistry common to the phosphite and phosphine complexes, but even here the chemistry is in substance quite different. The chemistry based on triphenylphosphine[9] is summarized in Scheme I. All the complexes cited in the scheme above with the exception of $HRh(CO)[P(C_6H_5)_3]_2$ have been generated as analogues in the phosphite system for the reactions of CO with $(\mu\text{-}H)_2Rh_2[P(O\text{-}i\text{-}C_3H_7)_3]_4$. Beyond this point, however, the similarities end. In the phosphite system, the CO ligand is relatively loosely bound whereas in the phosphine system a phosphine ligand is readily lost. Specifically, $HRh(CO)[P(C_6H_5)_3]_3$ reacts through phosphine ligand dissociation whereas the phosphite analogue reacts through CO ligand dissociation. Carbon monoxide reversibly reacts with $HRh(CO)[P(C_6H_5)_3]_3$ to form first $HRh(CO)_2[P(C_6H_5)_3]_2$ and then $Rh_2(\mu\text{-}CO)_4[P(C_6H_5)_3]_4$. Such transformations do not occur for $HRh(CO)[P(O\text{-}i\text{-}C_3H_7)_3]_3$. In addition, the interconvertible dimers $Rh_2(\mu\text{-}CO)_2[P(O\text{-}i\text{-}C_3H_7)_3]_4$ and $Rh_2(\mu\text{-}CO)_4[P(O\text{-}i\text{-}C_3H_7)_3]_4$ cannot be transformed by hydrogen to $HRh(CO)_2[P(O\text{-}i\text{-}C_3H_7)_3]_2$. Consistently and again in sharp contrast to the phosphine chemistry, the CO ligand in $HRh(CO)[P(O\text{-}i\text{-}C_3H_7)_3]_3$ is readily displaced to give $HRh[P(OR)_3]_4$ complexes. Clearly, the propensity for CO ligand loss in the phosphite system incisively differentiates this system from the phosphine system where phosphine ligand dissociation is the distinguishing chemical property. Also it is important to note that CO itself does not effect fragmentation of the rhodium dimer rather as shown in Figure 2 it probably is a phosphite ligand, lost from the intermediate **2**, that is responsible for the dimer fragmentation.

Table II. Selected Intramolecular Distances (Å) and Angles (Deg) for $Rh_2(\mu\text{-}CO)_2[P(O\text{-}i\text{-}C_3H_7)_3]_4$

| | | | |
|---|---|---|---|
| (a) Distances from the Rh Atom | | | |
| Rh-Rh[a] | 2.630 (1) | Rh-C | 2.013 (8) |
| Rh-P(1) | 2.256 (2) | Rh-C' | 2.054 (8) |
| Rh-P(2) | 2.253 (2) | | |
| (b) Distances within the Ligands | | | |
| C-O | 1.141 (8) | C(1)-C(2) | 1.538 (15) |
| P(1)-O(1) | 1.590 (6) | C(1)-C(3) | 1.561 (14) |
| P(1)-O(2) | 1.574 (6) | C(4)-C(5) | 1.538 (14) |
| P(1)-O(3) | 1.611 (6) | C(4)-C(6) | 1.533 (15) |
| P(2)-O(4) | 1.568 (5) | C(7)-C(8) | 1.480 (17) |
| P(2)-O(5) | 1.594 (11) | C(7)-C(9) | 1.435 (17) |
| P(2)-O(6) | 1.651 (13) | C(10)-C(11) | 1.516 (22) |
| O(1)-C(1) | 1.478 (10) | C(10)-C(12) | 1.495 (22) |
| O(2)-C(4) | 1.502 (10) | C(13)-C(14) | 1.522 (20) |
| O(3)-C(7) | 1.447 (13) | C(13)-C(15) | 1.521 (18) |
| O(4)-C(10) | 1.494 (11) | C(16)-C(17) | 1.442 (19) |
| O(5)-C(13) | 1.437 (18) | C(16)-C(18) | 1.395 (24) |
| O(6)-C(16) | 1.344 (20) | | |
| (c) Angles about the Rh Atom | | | |
| P(1)-Rh-P(2) | 98.88 (9) | Rh-C-O | 148.8 (7) |
| P(1)-Rh-C | 151.0 (2) | Rh'-C-O | 130.5 (7) |
| P(1)-Rh-C' | 94.7 (2) | Rh-P(1)-O(1) | 110.7 (3) |
| P(1)-Rh-Rh' | 117.33 (6) | Rh-P(1)-O(2) | 123.9 (2) |
| P(2)-Rh-C | 97.1 (2) | Rh-P(1)-O(3) | 110.6 (3) |
| P(2)-Rh-C' | 133.0 (2) | Rh-P(2)-O(4) | 117.6 (3) |
| P(2)-Rh-Rh' | 143.79 (8) | Rh-P(2)-O(5) | 118.1 (4) |
| C-Rh-C' | 90.9 (4) | Rh-P(2)-O(6) | 116.6 (5) |
| (d) Angles Associated with the Phosphite Ligands | | | |
| O(1)-P(1)-O(2) | 105.5 (3) | O(2)-C(4)-C(6) | 105.3 (10) |
| O(1)-P(1)-O(3) | 97.4 (3) | O(3)-C(7)-C(8) | 111.9 (11) |
| O(2)-P(1)-O(3) | 98.1 (4) | O(3)-C(7)-C(9) | 106.1 (14) |
| O(4)-P(2)-O(5) | 105.1 (5) | O(4)-C(10)-C(11) | 105.3 (13) |
| O(4)-P(2)-O(6) | 96.5 (4) | O(4)-C(10)-C(12) | 106.2 (14) |
| O(5)-P(2)-O(6) | 96.5 (7) | O(5)-C(13)-C(14) | 107.4 (14) |
| P(1)-O(1)-C(1) | 120.9 (7) | O(5)-C(13)-C(15) | 106.5 (15) |
| P(1)-O(2)-C(4) | 126.5 (5) | O(6)-C(16)-C(17) | 110.6 (14) |
| P(1)-O(3)-C(7) | 124.2 (6) | O(6)-C(16)-C(18) | 106.8 (23) |
| P(2)-O(4)-C(10) | 122.0 (7) | C(2)-C(1)-C(3) | 111.9 (11) |
| P(2)-O(5)-C(13) | 125.2 (8) | C(5)-C(4)-C(6) | 112.7 (9) |
| P(2)-O(6)-C(16) | 125.9 (9) | C(8)-C(7)-C(9) | 111.5 (12) |
| O(1)-C(1)-C(2) | 104.8 (9) | C(11)-C(10)-C(12) | 109.8 (13) |
| O(1)-C(1)-C(3) | 105.2 (10) | C(14)-C(13)-C(15) | 116.2 (15) |
| O(2)-C(4)-C(5) | 106.1 (9) | C(17)-C(16)-C(18) | 99.8 (17) |
| (e) Dihedral Angles between Planes Defined by Three Atoms | | | |
| Rh-Rh'-C and Rh-Rh'-C' | 140.8 (6) | | |
| Rh-C-C' and Rh'-C-C' | 136.8 (5) | | |
| Rh-P(1)-P(2) and Rh-C-C' | 53.6 (2) | | |
| Rh-P(1)-C and Rh-P(2)-C' | 126.7 (2) | | |
| Rh-P(1)-P(2) and Rh'-P(1)'-P(2)' | 77.9 (1) | | |

[a] The coordinates of primed atoms have been transformed by $(-x, y, {}^1/_2 - z)$.

**Description of the Structure of $Rh_2(\mu\text{-}CO)_2[P(O\text{-}i\text{-}C_3H_7)_3]_4$.** An ORTEP drawing of the framework atoms of $Rh_2(\mu\text{-}CO)_2[P(O\text{-}i\text{-}C_3H_7)_3]_4$ is presented in Figure 3. Atomic coordinates and anisotropic thermal parameters for the nonhydrogen atoms are listed in Table I; important bond distances and bond angles are compiled in Table II. A stereoview of $Rh_2(\mu\text{-}CO)_2[P(O\text{-}i\text{-}C_3H_7)_3]_4$ is included in the supplementary material (Figure 4).

Although the structure of $Rh_2(\mu\text{-}CO)_2[P(O\text{-}i\text{-}C_3H_7)_3]_4$ cannot be understood in terms of simple polyhedra, the structure can be derived from distortions of the corresponding hypothetical molecule in which all of the ligating atoms and the two rhodium atoms lie in the same plane. Twisting the Rh–P(1)–P(2) and Rh'–P'(1)–P'(2) planes to a dihedral angle of 77.9° and moving the two carbonyl groups about the rhodium–rhodium bond toward the same side of the molecule in such a way as to preserve a twofold axis of symmetry perpendicular to the rhodium–rhodium bond generates the observed structure. The dihedral angle between Rh–Rh'–C and Rh–Rh'–C' planes is then 140.8 (6)°. We have

previously pointed out that such a distortion should have a low-energy barrier for compounds of formulation $Rh_2(\mu\text{-}L)_2L'_4$ based on zero-valent rhodium atoms.[14] The structure of this molecule is essentially the same as what was previously reported for $Rh_2(\mu\text{-}CO)_2[P(C_6H_5)_3]_4$,[15] except for the fact that the latter crystal structure included two $CH_2Cl_2$ solvent molecules which were within bonding distance of the carbonyl ligands. This solvent interaction resulted in a somewhat elongated carbon-oxygen bonding distance in the phosphine complex compared to the phosphite complex (1.175 (8) Å vs. 1.141 (8) Å, respectively). In the solution state, the solvent molecules were shown to occupy a discrete coordination site, inducing one bridging carbonyl to move to a terminal position. Aside from this solvent interaction, the difference between these two structures can be explained by the larger steric requirement of the $P(C_6H_5)_3$ ligand. For example, the P-Rh-P angle is 103.71 (1)° in the triphenylphosphine complex compared to 98.99 (9)° in the phosphite complex. The rhodium-phosphorus bond distances are significantly shorter in the phosphite compound than in the triphenylphosphine compound (2.253 (2) and 2.256 (2) Å vs. 2.321 (2) and 2.327 (2) Å). This fact is reflective of the more effective bonding of the phosphite ligand to the low-valent metal irrespective of electronic or steric interpretations, a structural feature fully consistent with the chemistries of the phosphite- and phosphine-based rhodium systems. Otherwise, the pertinent features of the structures are the same: Rh-Rh = 2.630 (1) Å, Rh-C = 2.013 (8) Å, and Rh'-C = 2.054 (8) Å for the phosphite complex; Rh-Rh = 2.630 (1) Å, Rh-C = 2.051 (6) Å, and Rh'-C = 1.956 (7) Å for the phosphine complex.

**Acknowledgment.** This collaborative research was supported by the National Science Foundation (Grant CHE-78-08711). All work at Argonne National Laboratory was performed under the auspices of the Division of Basic Energy Sciences of the U.S. Department of Energy. The rhodium chloride used in these studies was obtained on a loan grant from Johnson Matthey, Inc. We also thank the Miller Institute for Basic Research in Science for a grant in the form of a Miller Professorship (to E.L.M.).

**Supplementary Material Available:** A stereoview of $Rh_2(\mu\text{-}CO)_2[P(O\text{-}i\text{-}C_3H_7)_3]_4$ (Figure 4) and a listing of the observed and calculated structure factor amplitudes (5 pages). Ordering information is given on any current masthead page.

(14) Teller, R. G.; Williams, J. M.; Koetzle, T. F.; Burch, R. R.; Gavin, R. M.; Muetterties, E. L. *Inorg. Chem.* **1981**, *20*, 1806.
(15) Singh, P.; Dammann, C. B.; Hodgson, D. J. *Inorg. Chem.* **1973**, *12*, 1335.

# The Reaction between Sulfur Dioxide and Hexamethyldisilazane. 3. The Characterization of Ammonium (Trimethylsilyl)sulfite

**D. W. Bennett† and L. D. Spicer***

*Contribution from the Department of Chemistry, University of Utah, Salt Lake City, Utah 84112.* *Received November 26, 1980. Revised Manuscript Received April 20, 1981*

**Abstract:** The reaction between $((CH_3)_3Si)_2NH$ and $SO_2$ results in the formation of an ionic solid with empirical formula $NH_4(CH_3)_3SiOSO_2$ which readily "sublimes" at ambient temperature. Although (trimethylsilyl)ammonium bisulfite is a logical choice for a molecular formula, IR, NMR, and XPS data rule out the presence of $RNH_3^+$ and $HSO_3^-$ ions. These data, along with a consideration of the solution behavior of this unique material, provide strong evidence that the substance is ammonium (trimethylsilyl)sulfite, with the silicon bonded to oxygen rather than sulfur.

In a recent paper[1] we reported the formation of a unique "sublimable" ionic solid from the reaction of sulfur dioxide with hexamethyldisilazane. This deceptively simple reaction occurs rapidly at temperatures below 0 °C to produce $((CH_3)_3Si)_2O$, $(CH_3)_3SiNSO$, and the solid of interest here. The solid formed contains one trimethylsilyl group per mole and has an empirical formala: $C_3H_{13}NO_3SSi$ (**1**). In addition the facile sublimation of this solid makes it an excellent model system in which to study solid-vapor equilibria of inorganic, ionic systems of this type. It should also be noted that this new compound has synthetic utility as a source of silanol, ammonia, and sulfur dioxide, all of which can be generated in situ by gently heating the solid.[1b] While the reaction chemistry of **1** remains to be investigated, the evidence contained herein suggests that the $(CH_3)_3SiOSO_2^-$ is present in alcohol and $Me_2SO$ solutions, probably providing either the (trimethylsilyl)sulfite ion or $(CH_3)_3SiO^-$, an alkoxide analogue, as synthetic intermediates. Because of its interesting physical properties and potential synthetic utility, we have undertaken the task of characterizing this novel substance.

The nature of the $((CH_3)_3Si)_2NH/SO_2$ reaction, coupled with the volatility of the solid, led us to speculate that it was either a (trimethylsilyl)ammonium bisulfite, $(CH_3)_3SiNH_3HSO_3$ or an ammonium (trimethylsilyl)sulfite, $NH_4(CH_3)_3SiOSO_2$. Ammonium (trimethylsilyl)sulfonate, $(CH_3)_3SiSO_3NH_4$, is also a possible structure although the mechanism proposed and thermochemistry suggest the sulfite is preferred.

Of the three possibilities, the sulfite is perhaps the most attractive candidate consistent with a rather complex reaction scheme proposed for the $SO_2/((CH_3)_3Si)_2NH$ reaction.[1] While sublimation properties, reaction stoichiometry, and feasibility of formation appear to make the bisulfite a less likely candidate, definitive evidence to confirm this postulate has not yet been reported due to the unusual physical properties of the solid which make it difficult to handle quantitatively. In addition, as an ammonium salt the solid might be expected to exist as a sulfonate based on organic analogues, but the relative bond energies of silicon-oxygen vs. silicon-sulfur suggest that sulfite formation would be favored. Several attempts to obtain X-ray crystallographic data on **1** have failed, making it necessary to resort to reaction chemistry, conductivity studies, vapor pressure data, and

† Department of Chemistry and Geology, Clemson University.

(1) (a) Davis, J. F.; Spicer, L. D. *Inorg. Chem.* **1980**, *19*, 2191. Bennett, D. W.; Spicer, L. D. paper 2 in this series, submitted for publication. (b) The vapor-phase chemistry of **1** will be described in a later paper.

0002-7863/81/1503-5522$01.25/0 